Draft version February 25, 2018
Typeset using LaTeX **modern** style in AASTeX61

STARRY: ANALYTIC OCCULTATION LIGHT CURVES

Rodrigo Luger[1] and others

[1] *Department of Astronomy, University of Washington, Seattle, WA*

ABSTRACT

We derive analytical, closed form solutions for the total flux received from a planet, moon or star during an occultation if the specific intensity map of the body is expressed as a sum of spherical harmonics. Our expressions are valid to arbitrary order and may be computed recursively for speed. The formalism we develop here applies to the computation of stellar transit light curves, planetary secondary eclipse light curves, and planet-planet/planet-moon occultation light curves, as well as rotational phase curves. We present starry, a full photodynamical code written in C and wrapped in Python that computes these light curves. starry also computes analytic derivatives of the light curves with respect to all input parameters for use in gradient-based inference schemes such as Hamiltonian monte carlo (HMC), allowing users to quickly and efficiently regress on observed light curves to infer properties of a celestial body's surface map.

Keywords: methods: analytical — techniques: photometric

1. INTRODUCTION

We provide links to Python code ( ) to reproduce all figures in this paper, as well as links to Mathematica scripts ( ) containing proofs and derivations of the principal equations. For convenience, Table 1 at the end lists all the symbols used in the paper, with references to the equations defining them.

todo

2. SPHERICAL HARMONICS

The real spherical harmonic $Y_{lm}(\theta, \phi)$ of order l and degree m is defined in spherical coordinates as

$$Y_{lm}(\theta, \phi) = \begin{cases} \bar{P}_{lm}(\cos\theta)\cos(m\phi) & m \geq 0 \\ \bar{P}_{l|m|}(\cos\theta)\sin(|m|\phi) & m < 0\,, \end{cases} \tag{1}$$

where $\bar{P}_{lm}$ is the normalized associated Legendre function. On the surface of the unit sphere, we have

$$\begin{aligned} x &= \sin\theta\cos\phi \\ y &= \sin\theta\sin\phi \\ z &= \cos\theta\,. \end{aligned} \tag{2}$$

Expanding Equation (1) using the multiple angle formula, we obtain

$$Y_{lm}(x, y, z) = \left(\frac{1}{\sqrt{1-z^2}}\right)^m \begin{cases} \bar{P}_{lm}(z) \displaystyle\sum_{j \text{ even}}^{m} (-1)^{\frac{j}{2}} \binom{m}{j} x^{m-j} y^j & m \geq 0 \\ \bar{P}_{l|m|}(z) \displaystyle\sum_{j \text{ odd}}^{m} (-1)^{\frac{j-1}{2}} \binom{m}{j} x^{m-j} y^j & m < 0\,, \end{cases} \tag{3}$$

where $\binom{\cdot}{\cdot}$ is the binomial coefficient. The normalized associated Legendre function is defined as

$$\bar{P}_{lm}(z) = A_{lm} \left(\sqrt{1-z^2}\right)^m \frac{\mathrm{d}^m}{\mathrm{d}z^m} \left[\frac{1}{2^l l!} \frac{\mathrm{d}^l}{\mathrm{d}z^l} \left(z^2-1\right)^l\right]\,, \tag{4}$$

where

$$A_{lm} = \sqrt{\frac{(2-\delta_{m0})(2l+1)(l-m)!}{4\pi(l+m)!}}\,. \tag{5}$$

Expanding out the z derivatives, we obtain

$$\bar{P}_{lm}(z) = A_{lm}\left(\sqrt{1-z^2}\right)^m \sum_{k=0}^{l-m} \frac{2^l\left(\frac{l+m+k-1}{2}\right)!}{k!(l-m-k)!\left(\frac{-l+m+k-1}{2}\right)!} z^k\,, \tag{6}$$

which we combine with the previous results to write

$$Y_{lm}(x,y,z) = \begin{cases} \displaystyle\sum_{j\,\mathrm{even}}^{m}\sum_{k=0}^{l-m}(-1)^{\frac{j}{2}}\,A_{lm}B_{lm}^{jk}x^{m-j}y^j z^k & m \geq 0 \\ \displaystyle\sum_{j\,\mathrm{odd}}^{|m|}\sum_{k=0}^{l-|m|}(-1)^{\frac{j-1}{2}}\,A_{l|m|}B_{l|m|}^{jk}x^{|m|-j}y^j z^k & m < 0 \end{cases} \tag{7}$$

where

$$B_{lm}^{jk} = \frac{2^l m!\left(\frac{l+m+k-1}{2}\right)!}{j!k!(m-j)!(l-m-k)!\left(\frac{-l+m+k-1}{2}\right)!}\,. \tag{8}$$

Since we are confined to the surface of the unit sphere, we have $z = \sqrt{1-x^2-y^2}$ and we may expand z^k using the binomial theorem:

$$\begin{aligned} z^k &= (1-x^2-y^2)^{\frac{k}{2}} \\ &= \begin{cases} \displaystyle\sum_{p\,\mathrm{even}}^{k}\sum_{q\,\mathrm{even}}^{p}(-1)^{\frac{p}{2}}C_{pq}^{k}x^{p-q}y^q & k\,\mathrm{even} \\ \displaystyle\sum_{p\,\mathrm{even}}^{k-1}\sum_{q\,\mathrm{even}}^{p}(-1)^{\frac{p}{2}}C_{pq}^{k-1}x^{p-q}y^q\sqrt{1-x^2-y^2} & k\,\mathrm{odd}\,, \end{cases} \end{aligned} \tag{9}$$

where

$$C_{pq}^{k} = \frac{\left(\frac{k}{2}\right)!}{\left(\frac{q}{2}\right)!\left(\frac{k-p}{2}\right)!\left(\frac{p-q}{2}\right)!}\,. \tag{10}$$

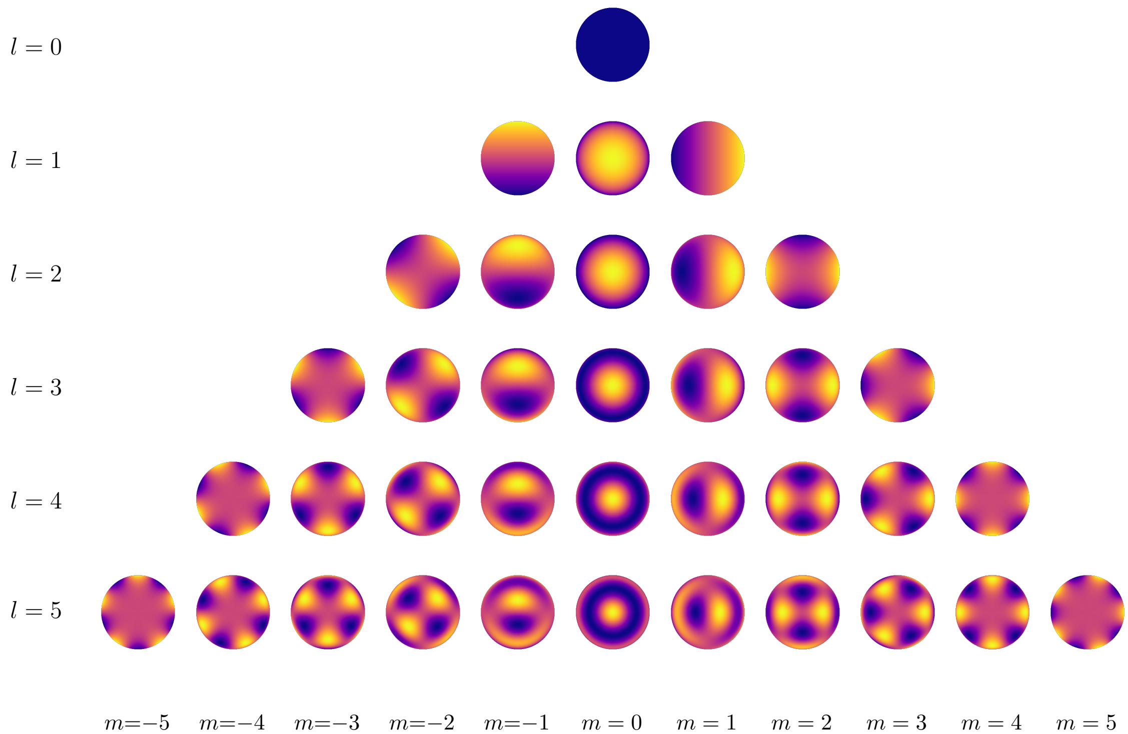

Figure 1. The real spherical harmonics up to order $l = 5$ computed from Equation (11). In these plots, the x-axis points to the right, the y-axis points up, and the z-axis points out of the page. An animated version can be viewed here.

This gives us an expression for the spherical harmonic Y_{lm} as a function of x and y only:

$$
Y_{lm}(x,y) = \begin{cases}
\displaystyle\sum_{j\,\mathrm{even}}^{m} \sum_{k\,\mathrm{even}}^{l-m} \sum_{p\,\mathrm{even}}^{k} \sum_{q\,\mathrm{even}}^{p} (-1)^{\frac{j+p}{2}} A_{lm} B_{lm}^{jk} C_{pq}^{k} x^{m-j+p-q} y^{j+q} + & \\
\displaystyle\sum_{j\,\mathrm{even}}^{m} \sum_{k\,\mathrm{odd}}^{l-m} \sum_{p\,\mathrm{even}}^{k-1} \sum_{q\,\mathrm{even}}^{p} (-1)^{\frac{j+p}{2}} A_{lm} B_{lm}^{jk} C_{pq}^{k-1} x^{m-j+p-q} y^{j+q} z & m \geq 0 \\
& \\
\displaystyle\sum_{j\,\mathrm{odd}}^{|m|} \sum_{k\,\mathrm{even}}^{l-|m|} \sum_{p\,\mathrm{even}}^{k} \sum_{q\,\mathrm{even}}^{p} (-1)^{\frac{j+p-1}{2}} A_{l|m|} B_{l|m|}^{jk} C_{pq}^{k} x^{|m|-j+p-q} y^{j+q} + & \\
\displaystyle\sum_{j\,\mathrm{odd}}^{|m|} \sum_{k\,\mathrm{odd}}^{l-|m|} \sum_{p\,\mathrm{even}}^{k-1} \sum_{q\,\mathrm{even}}^{p} (-1)^{\frac{j+p-1}{2}} A_{l|m|} B_{l|m|}^{jk} C_{pq}^{k-1} x^{|m|-j+p-q} y^{j+q} z & m < 0
\end{cases} \tag{11}
$$

where $z = z(x,y) = \sqrt{1-x^2-y^2}$.

3. SURFACE MAP VECTORS

We represent a surface map as a vector $\mathbf{y}$ of spherical harmonic coefficients such that the specific intensity at the point (x, y) may be written

$$I(x, y) = \tilde{\mathbf{y}}^\mathsf{T}(x, y)\,\mathbf{y}\,, \tag{12}$$

where $\tilde{\mathbf{y}}$ is the basis of spherical harmonics, arranged in increasing degree and order:

$$\tilde{\mathbf{y}} = \begin{pmatrix} Y_{0,0} & Y_{1,-1} & Y_{1,0} & Y_{1,1} & Y_{2,-2} & Y_{2,-1} & Y_{2,0} & Y_{2,1} & Y_{2,2} & \cdots \end{pmatrix}^\mathsf{T}\,, \tag{13}$$

where $Y_{l,m} = Y_{l,m}(x, y)$ are given by Equation (11). For reference, in this basis the coefficient of the spherical harmonic $Y_{l,m}$ is located at the index

$$n = l^2 + l + m \tag{14}$$

of the vector $\mathbf{y}$. Conversely, the coefficient at index n of $\mathbf{y}$ corresponds to the spherical harmonic of order and degree given by

$$\begin{aligned} l &= \left\lfloor \sqrt{n} \right\rfloor \\ m &= n - \left\lfloor \sqrt{n} \right\rfloor^2 - \left\lfloor \sqrt{n} \right\rfloor\,. \end{aligned} \tag{15}$$

4. ROTATION

4.1. *Euler angles*

Defining a map as a vector of spherical harmonic coefficients makes it straightforward to compute the projection of the map under arbitrary rotations of the body via a rotation matrix $\mathbf{R}$:

$$\mathbf{y}' = \mathbf{R}\,\mathbf{y} \tag{16}$$

where $\mathbf{y}'$ are the spherical harmonic coefficients of the rotated map. Collado et al. (1989) derived expressions for the rotation matrices for the real spherical harmonics of a given order l from the corresponding complex rotation matrices (Steinborn & Ruedenberg 1973):

$$\mathbf{R}^l = \mathbf{U}^{-1}\mathbf{D}^l\mathbf{U} \tag{17}$$

where

$$
\begin{aligned}
\mathbf{D}^{l}_{m,m'} &= \mathrm{e}^{-\mathbf{i}(\alpha m'+\gamma m)}(-1)^{m'+m}\sqrt{(l-m)!(l+m)!(l-m')!(l+m')!} \\
&\quad \times \sum_{k}(-1)^{k}\frac{\cos\left(\frac{\beta}{2}\right)^{2l+m-m'-2k}\sin\left(\frac{\beta}{2}\right)^{-m+m'+2k}}{k!(l+m-k)!(l-m'-k)!(m'-m+k)!}
\end{aligned}
\tag{18}
$$

is the rotation matrix for the complex spherical harmonics of order l and

$$
\mathbf{U} = \frac{1}{\sqrt{2}}
\begin{pmatrix}
\ddots & & & & & & & & \iddots \\
 & \mathbf{i} & & & & & & 1 & \\
 & & \mathbf{i} & & & & 1 & & \\
 & & & \mathbf{i} & & 1 & & & \\
 & & & & \sqrt{2} & & & & \\
 & & & \mathbf{i} & & -1 & & & \\
 & & -\mathbf{i} & & & & 1 & & \\
 & \mathbf{i} & & & & & & -1 & \\
\iddots & & & & & & & & \ddots
\end{pmatrix}.
\tag{19}
$$

describes the transformation from complex to real spherical harmonics. In Equation (18) above, α, β, and γ are the (proper) Euler angles for rotation in the $z-y-z$ convention. To obtain a rotation matrix for an arbitrary vector $\mathbf{y}$ with spherical harmonics of different orders up to $l = l_{\max}$, we define the block-diagonal matrix $\mathbf{R}$:

$$
\mathbf{R} =
\begin{pmatrix}
\mathbf{R}^{0} & & & & \\
 & \mathbf{R}^{1} & & & \\
 & & \mathbf{R}^{2} & & \\
 & & & \mathbf{R}^{3} & \\
 & & & & \ddots
\end{pmatrix}.
\tag{20}
$$

Rotation of $\mathbf{y}$ by the Euler angles α, β, and γ is performed via Equation (16) with $\mathbf{R}$ given by Equation (20).

4.2. *Axis-angle*

It is often more convenient to define a rotation by an axis $\mathbf{u}$ and an angle θ of rotation about that axis. Given a unit vector $\mathbf{u}$ and an angle θ, we can find the corresponding Euler angles by comparing the 3-dimensional Cartesian rotation matrices for both systems,

$$\mathbf{P} = \begin{pmatrix} c_\theta + u_x^2\,(1-c_\theta) & u_x u_y\,(1-c_\theta) - u_z s_\theta & u_x u_z\,(1-c_\theta) + u_y s_\theta \\ u_y u_x\,(1-c_\theta) + u_z s_\theta & c_\theta + u_y^2\,(1-c_\theta) & u_y u_z\,(1-c_\theta) - u_x s_\theta \\ u_z u_x\,(1-c_\theta) - u_y s_\theta & u_z u_y\,(1-c_\theta) + u_x s_\theta & c_\theta + u_z^2\,(1-c_\theta) \end{pmatrix} \tag{21}$$

for axis-angle rotations and

$$\mathbf{Q} = \begin{pmatrix} c_\alpha c_\beta c_\gamma - s_\alpha s_\gamma & -c_\gamma s_\alpha - c_\alpha c_\beta s_\gamma & c_\alpha s_\beta \\ c_\alpha s_\gamma + c_\beta c_\gamma s_\alpha & c_\alpha c_\gamma - c_\beta s_\alpha s_\gamma & s_\alpha s_\beta \\ -c_\gamma s_\beta & s_\beta s_\gamma & c_\beta \end{pmatrix}, \tag{22}$$

for Euler rotations, where $c_\cdot \equiv \cos(\cdot)$ and $s_\cdot \equiv \sin(\cdot)$. Comparison of the two matrices gives us expressions for the Euler angles in terms of $\mathbf{u}$ and θ:

$$\begin{aligned} \cos\alpha &= \tfrac{P_{0,2}}{\sqrt{P_{0,2}^2+P_{1,2}^2}} & \cos\beta &= P_{2,2} & \cos\gamma &= -\tfrac{P_{2,0}}{\sqrt{P_{2,0}^2+P_{2,1}^2}} \\ \sin\alpha &= \tfrac{P_{1,2}}{\sqrt{P_{0,2}^2+P_{1,2}^2}} & \sin\beta &= \sqrt{1-P_{2,2}^2} & \sin\gamma &= \tfrac{P_{2,1}}{\sqrt{P_{2,0}^2+P_{2,1}^2}} \end{aligned}. \tag{23}$$

Thus, given a spherical harmonic vector $\mathbf{y}$, we can calculate how it transforms under rotation by an angle θ about an axis $\mathbf{u}$ by first computing the Euler angles (Equation 23) and using those to construct the spherical harmonic rotation matrix (Equation 20).

5. CHANGE OF BASIS

5.1. *Polynomial basis*

In order to compute the occultation light curve for a body with a given surface map $\mathbf{y}$, it is convenient to first find its polynomial representation $\mathbf{p}$, which we express as a vector of coefficients in the polynomial basis $\tilde{\mathbf{p}}$:

$$\begin{aligned} \tilde{p}_n &= \begin{cases} x^{\frac{\mu}{2}} y^{\frac{\nu}{2}} & \nu \text{ even} \\ x^{\frac{\mu-1}{2}} y^{\frac{\nu-1}{2}} z & \nu \text{ odd} \end{cases} \\ \tilde{\mathbf{p}} &= \begin{pmatrix} 1 & x & z & y & x^2 & xz & xy & yz & y^2 & \cdots \end{pmatrix}^\mathsf{T}, \end{aligned} \tag{24}$$

where

$$\begin{aligned} \mu &= l - m \\ \nu &= l + m \end{aligned} \tag{25}$$

with l and m given by Equation (15). To find $\mathbf{p}$ given $\mathbf{y}$, we introduce the change of basis matrix $\mathbf{A_1}$, which transforms a vector in the spherical harmonic basis $\tilde{\mathbf{y}}$ to the polynomial basis $\tilde{\mathbf{p}}$:

$$\mathbf{p} = \mathbf{A_1}\,\mathbf{y} \tag{26}$$

The columns of $\mathbf{A_1}$ are simply the polynomial vectors corresponding to each of the spherical harmonics in Equation (13). From Equations (11) and (24), we can calculate the first few spherical harmonics and their corresponding polynomial vectors:

$$\begin{aligned}
Y_{0,0} &= \tfrac{1}{2\sqrt{\pi}} & \mathbf{p} &= \tfrac{1}{2\sqrt{\pi}}\begin{pmatrix}1 & 0 & 0 & 0 & \cdots\end{pmatrix}^\mathsf{T} \\
Y_{1,-1} &= \tfrac{\sqrt{3}}{2\sqrt{\pi}}y & \mathbf{p} &= \tfrac{1}{2\sqrt{\pi}}\begin{pmatrix}0 & 0 & 0 & \sqrt{3} & \cdots\end{pmatrix}^\mathsf{T} \\
Y_{1,0} &= \tfrac{\sqrt{3}}{2\sqrt{\pi}}z & \mathbf{p} &= \tfrac{1}{2\sqrt{\pi}}\begin{pmatrix}0 & 0 & \sqrt{3} & 0 & \cdots\end{pmatrix}^\mathsf{T} \\
Y_{1,1} &= \tfrac{\sqrt{3}}{2\sqrt{\pi}}x & \mathbf{p} &= \tfrac{1}{2\sqrt{\pi}}\begin{pmatrix}0 & \sqrt{3} & 0 & 0 & \cdots\end{pmatrix}^\mathsf{T} \\
Y_{2,-2} &= \cdots & \mathbf{p} &= \cdots
\end{aligned} \tag{27}$$

From these we can construct $\mathbf{A_1}$. As an example, for spherical harmonics up to order $l_{\max} = 2$, this is

$$\mathbf{A_1} = \frac{1}{2\sqrt{\pi}}\begin{pmatrix}
1 & 0 & 0 & 0 & 0 & 0 & \sqrt{5} & 0 & 0 \\
0 & 0 & 0 & \sqrt{3} & 0 & 0 & 0 & 0 & 0 \\
0 & 0 & \sqrt{3} & 0 & 0 & 0 & 0 & 0 & 0 \\
0 & \sqrt{3} & 0 & 0 & 0 & 0 & 0 & 0 & 0 \\
0 & 0 & 0 & 0 & 0 & 0 & -\frac{3\sqrt{5}}{2} & 0 & \frac{\sqrt{15}}{2} \\
0 & 0 & 0 & 0 & 0 & 0 & 0 & \sqrt{15} & 0 \\
0 & 0 & 0 & 0 & \sqrt{15} & 0 & 0 & 0 & 0 \\
0 & 0 & 0 & 0 & 0 & \sqrt{15} & 0 & 0 & 0 \\
0 & 0 & 0 & 0 & 0 & 0 & -\frac{3\sqrt{5}}{2} & 0 & -\frac{\sqrt{15}}{2}
\end{pmatrix}. \tag{28}$$

As before, the specific intensity at the point (x, y) may be computed as

$$\begin{aligned}
I(x, y) &= \tilde{\mathbf{p}}^\mathsf{T}\mathbf{p} \\
&= \tilde{\mathbf{p}}^\mathsf{T}\mathbf{A_1}\,\mathbf{y}\,.
\end{aligned} \tag{29}$$

5.2. *Green's basis*

As we will see in the next section, integrating the surface map over the disk of the body is easier if we apply one final transformation to our input vector, rotating it into what we will refer to as the *Green's basis*, $\tilde{\mathbf{g}}$:

$$\tilde{g}_n = \begin{cases} \frac{\mu+2}{2} x^{\frac{\mu}{2}} y^{\frac{\nu}{2}} & \nu \text{ even} \\ z & \nu = \mu = 1 \\ 3x^{l-2}yz & \nu \text{ odd},\ \mu = 1,\ l \text{ even} \\ z\Big(-x^{l-3} + x^{l-1} + 4x^{l-3}y^2\Big) & \nu \text{ odd},\ \mu = 1,\ l \text{ odd} \\ z\Big(\frac{\mu-3}{2} x^{\frac{\mu-5}{2}} y^{\frac{\nu-1}{2}} - \frac{\mu-3}{2} x^{\frac{\mu-5}{2}} y^{\frac{\nu+3}{2}} - \frac{\mu+3}{2} x^{\frac{\mu-1}{2}} y^{\frac{\nu-1}{2}}\Big) & \text{otherwise} \end{cases}$$

$$\tilde{\mathbf{g}} = \begin{pmatrix} 1 & 2x & z & y & 3x^2 & -3xz & 2xy & 3yz & y^2 & \cdots \end{pmatrix}^\mathsf{T}, \tag{30}$$

where the values of l, m, μ, and ν are given by Equations (15) and (25). Given a polynomial vector $\mathbf{p}$, the corresponding vector in the Green's basis, $\mathbf{g}$, can be found by performing another change of basis operation:

$$\mathbf{g} = \mathbf{A_2}\,\mathbf{p} \tag{31}$$

where the columns of the matrix $\mathbf{A_2}$ are the Green's vectors corresponding to each of the polynomial terms in Equation (24). In practice, it is easier to express the elements of $\tilde{\mathbf{g}}$ in terms of the elements of $\tilde{\mathbf{p}}$ and use those to populate the columns of the matrix $\mathbf{A_2}^{-1}$. Continuing our example for $l_{\max} = 2$, our second change of basis matrix is

$$\mathbf{A_2} = \begin{pmatrix} 1 & 0 & 0 & 0 & 0 & 0 & 0 & 0 & 0 \\ 0 & \frac{1}{2} & 0 & 0 & 0 & 0 & 0 & 0 & 0 \\ 0 & 0 & 1 & 0 & 0 & 0 & 0 & 0 & 0 \\ 0 & 0 & 0 & 1 & 0 & 0 & 0 & 0 & 0 \\ 0 & 0 & 0 & 0 & \frac{1}{3} & 0 & 0 & 0 & 0 \\ 0 & 0 & 0 & 0 & 0 & -\frac{1}{3} & 0 & 0 & 0 \\ 0 & 0 & 0 & 0 & 0 & 0 & \frac{1}{2} & 0 & 0 \\ 0 & 0 & 0 & 0 & 0 & 0 & 0 & \frac{1}{3} & 0 \\ 0 & 0 & 0 & 0 & 0 & 0 & 0 & 0 & 1 \end{pmatrix}. \tag{32}$$

Given $\mathbf{A_1}$ and $\mathbf{A_2}$, we can easily transform a spherical harmonic vector $\mathbf{y}$ to a Green's vector $\mathbf{g}$:

$$
\begin{aligned}
\mathbf{g} &= \mathbf{A_2}\,\mathbf{A_1}\,\mathbf{y} \\
&= \mathbf{A}\,\mathbf{y}
\end{aligned}
\tag{33}
$$

where

$$
\mathbf{A} \equiv \mathbf{A_2}\,\mathbf{A_1} \tag{34}
$$

is the full change of basis matrix. For $l_{\mathrm{max}} = 2$,

$$
\mathbf{A} = \frac{1}{2\sqrt{\pi}} \begin{pmatrix}
1 & 0 & 0 & 0 & 0 & 0 & \frac{\sqrt{5}}{2} & 0 & 0 \\
0 & 0 & 0 & \sqrt{3} & 0 & 0 & 0 & 0 & 0 \\
0 & 0 & \sqrt{3} & 0 & 0 & 0 & 0 & 0 & 0 \\
0 & \frac{\sqrt{3}}{2} & 0 & 0 & 0 & 0 & 0 & 0 & 0 \\
0 & 0 & 0 & 0 & 0 & 0 & -\frac{3\sqrt{5}}{4} & 0 & \frac{\sqrt{15}}{2} \\
0 & 0 & 0 & 0 & 0 & 0 & 0 & \sqrt{\frac{5}{3}} & 0 \\
0 & 0 & 0 & 0 & \sqrt{\frac{5}{3}} & 0 & 0 & 0 & 0 \\
0 & 0 & 0 & 0 & 0 & -\sqrt{\frac{5}{3}} & 0 & 0 & 0 \\
0 & 0 & 0 & 0 & 0 & 0 & -\frac{3\sqrt{5}}{4} & 0 & -\frac{\sqrt{15}}{2}
\end{pmatrix} . \tag{35}
$$

For completeness, we note that the specific intensity at a point on a map described by the spherical harmonic vector $\mathbf{y}$ is

$$
\begin{aligned}
I(x, y) &= \tilde{\mathbf{g}}^{\mathsf{T}}(x, y)\mathbf{g} \\
&= \tilde{\mathbf{g}}^{\mathsf{T}}(x, y)\mathbf{A}\,\mathbf{y}\,.
\end{aligned}
\tag{36}
$$

6. LIGHT CURVES

6.1. *Phase curves*

Consider a body of unit radius centered at the origin, with a surface map given by the spherical harmonic vector $\mathbf{y}$ viewed at an orientation specified by the rotation matrix $\mathbf{R}$, such that the specific intensity at a point (x, y) on the surface is

$$
\begin{aligned}
I(x, y) &= \tilde{\mathbf{y}}^{\mathsf{T}}(x, y)\mathbf{R}\,\mathbf{y} \\
&= \tilde{\mathbf{p}}^{\mathsf{T}}(x, y)\mathbf{A_1}\,\mathbf{R}\,\mathbf{y}
\end{aligned}
\tag{37}
$$

where $\tilde{\mathbf{p}}$ is the polynomial basis and $\mathbf{A_1}$ is the corresponding change-of-basis matrix (§5.1). The total flux radiated in the direction of the observer is obtained by integrating the specific intensity over a region S of the projected disk of the body:

$$
\begin{aligned}
F &= \oiint I(x,y)\,\mathrm{d}S \\
&= \oiint \tilde{\mathbf{p}}^\mathsf{T}(x,y)\mathbf{A_1}\,\mathbf{R}\,\mathbf{y}\,\mathrm{d}S \\
&= \mathbf{r}^\mathsf{T}\mathbf{A_1}\,\mathbf{R}\,\mathbf{y}\,,
\end{aligned}
\tag{38}
$$

where $\mathbf{r}$ is a column vector whose n^{th} component is given by

$$
r_n \equiv \oiint \tilde{p}_n(x,y)\,\mathrm{d}S\,. \tag{39}
$$

When the entire disk of the body is visible (i.e., when no occultation is occurring), this may be written

$$
\begin{aligned}
r_n &= \int_{-1}^{1}\int_{-\sqrt{1-x^2}}^{\sqrt{1+x^2}} \tilde{p}_n(x,y)\,\mathrm{d}y\,\mathrm{d}x \\
&= \begin{cases}
\dfrac{\Gamma\left(\frac{\mu}{4}+\frac{1}{2}\right)\Gamma\left(\frac{\nu}{4}+\frac{1}{2}\right)}{\Gamma\left(\frac{\mu+\nu}{4}+2\right)} & \dfrac{\mu}{2}\text{ even, }\dfrac{\nu}{2}\text{ even} \\[2ex]
\dfrac{\sqrt{\pi}}{2}\dfrac{\Gamma\left(\frac{\mu}{4}+\frac{1}{4}\right)\Gamma\left(\frac{\nu}{4}+\frac{1}{4}\right)}{\Gamma\left(\frac{\mu+\nu}{4}+2\right)} & \dfrac{\mu-1}{2}\text{ even, }\dfrac{\nu-1}{2}\text{ even} \\[2ex]
0 & \text{otherwise.}
\end{cases}
\end{aligned}
\tag{40}
$$

where $\Gamma(\cdot)$ is the gamma function. Equation (38) may be used to analytically compute the phase curve of a body with an arbitrary surface map. Since $\mathbf{r}$ and $\mathbf{B}$ are independent of the map coefficients or its orientation, these may be pre-computed for computational efficiency.

6.2. *Occultation light curves*

Note that the specific intensity at a point (x, y) on the surface of a body described by the map $\mathbf{y}$ may also be written as

$$
\begin{aligned}
I(x,y) &= \tilde{\mathbf{y}}^\mathsf{T}(x,y)\mathbf{R}\,\mathbf{y} \\
&= \tilde{\mathbf{g}}^\mathsf{T}(x,y)\mathbf{A}\,\mathbf{R}\,\mathbf{y}\,,
\end{aligned}
\tag{41}
$$

where $\tilde{\mathbf{g}}$ is the Greens basis and $\mathbf{A}$ is the full change of basis matrix (§5.2). As before, the total flux radiated in the direction of the observer is obtained by integrating the specific intensity over a region S of the projected disk of the body:

$$\begin{aligned} F &= \oiint I(x,y)\,\mathrm{d}S \\ &= \oiint \tilde{\mathbf{g}}^{\mathsf{T}}(x,y)\mathbf{A}\,\mathbf{R}\,\mathbf{y}\,\mathrm{d}S \\ &= \mathbf{s}^{\mathsf{T}}\mathbf{A}\,\mathbf{R}\,\mathbf{y}\ , \end{aligned} \tag{42}$$

where $\mathbf{s}$ is a column vector whose n^{th} component is given by

$$s_n \equiv \oiint \tilde{g}_n(x,y)\,\mathrm{d}S\,. \tag{43}$$

This time, suppose the body is occulted by another body of radius r centered at the point (x_0, y_0), so that the surface S over which the integral is taken is a function of r, x_0, and y_0. In general, the integrals in Equation (50) are difficult (and often impossible) to compute directly. One way to simplify the problem is to first perform a rotation through an angle

$$\omega = \frac{\pi}{2} - \mathrm{arctan2}(y_0, x_0) \tag{44}$$

about the z-axis ($\mathbf{u} = [0,0,1]$) so that the occultor lies along the $+y$-axis, with its center located a distance $b = \sqrt{x_0^2 + y_0^2}$ from the origin (see Figure 2). In this rotated frame, the limits of integration (the two points of intersection between the occultor and the occulted body, should they exist) are symmetric about the y-axis. If we define $\phi \in [-\pi/2,\ \pi/2]$ as the angular position of the right hand side intersection point relative to the occultor center, measured counter-clockwise from the $+x$ direction, the arc of the occultor that overlaps the occulted body extends from $\pi - \phi$ to $2\pi + \phi$ (see the Figure). Similarly, defining $\lambda \in [-\pi/2,\ \pi/2]$ as the angular position of the same point relative to the origin, the arc of the portion of the occulted body that is visible during the occultation extends from $\pi - \lambda$ to $2\pi + \lambda$ (see the Figure). For future reference, it can be shown that

$$\phi = \begin{cases} \arcsin\left(\dfrac{1 - r^2 - b^2}{2br}\right) & |1 - r| < b < 1 + r \\ \dfrac{\pi}{2} & b \le 1 - r \end{cases} \tag{45}$$

and

$$\lambda = \begin{cases} \arcsin\left(\dfrac{1-r^2+b^2}{2b}\right) & |1-r| < b < 1+r \\ \dfrac{\pi}{2} & b \le 1-r\,, \end{cases} \tag{46}$$

The case $b \le 1-r$ corresponds to an occultation during which the occultor is fully within the planet disk, so no points of intersection exist. In this case, we define ϕ such that the arc from $\pi - \phi$ to $2\pi + \phi$ spans the entire circumference of the occultor, and λ such that the arc from $\pi - \lambda$ to $2\pi + \lambda$ spans the entire circumference of the occulted body. Note that if $b \ge 1+r$, no occultation occurs and the flux may be computed as in §6.1, while if $b \le r-1$, the entire disk of the body is occulted and the total flux is zero.

The second trick we employ to solve Equation (50) is to use Green's theorem to express the surface integral of $\tilde{\mathbf{g}}_n$ as the line integral of a vector function $\mathbf{G}_n$ along the boundary of the same surface (Pál 2012):

$$s_n = \oiint \tilde{g}_n(x,y)\,\mathrm{d}S = \oint \mathbf{G}_n(x,y)\cdot\mathrm{d}\mathbf{r} \tag{47}$$

where $\mathbf{G}_n(x,y) = G_{nx}(x,y)\,\hat{\mathbf{x}} + G_{ny}(x,y)\,\hat{\mathbf{y}}$ is chosen such that

$$\mathbf{D}\wedge\mathbf{G}_n = \tilde{g}_n(x,y)\,. \tag{48}$$

The operation $\mathbf{D}\wedge\mathbf{G}_n$ denotes the *exterior derivative* of $\mathbf{G}_n$. In two-dimensional Cartesian coordinates, it is given by

$$\mathbf{D}\wedge\mathbf{G} \equiv \frac{\mathrm{d}G_{ny}}{\mathrm{d}x} - \frac{\mathrm{d}G_{nx}}{\mathrm{d}y}\,. \tag{49}$$

Thus, in order to compute s_n in Equation (47), we must (1) apply a rotation to our map $\mathbf{y}$ to align the occultor with the $+y$-axis; (2) find a vector function $\mathbf{G}_n$ whose exterior derivative is the n^{th} component of the vector basis $\tilde{\mathbf{g}}$ (Equation 30); and (3) integrate it along the boundary of the visible portion of the occulted body's surface. In general, for an occultation involving two bodies, this boundary consists of two arcs: a segment of the circle bounding the occultor (thick red curve in Figure 2), and a segment of the circle bounding the occulted body (thick black curve in Figure 2). If we happen to know $\mathbf{G}_n$, the integral in Equation (47) is just

$$s_n = \mathcal{P}(\mathbf{G}_n) - \mathcal{Q}(\mathbf{G}_n)\,, \tag{50}$$

where, as in Pál (2012), we define the *primitive integrals*

$$\mathcal{P}(\mathbf{G}_n) = \int\limits_{\pi-\phi}^{2\pi+\phi} \left[G_{ny}(rc_\varphi, b + rs_\varphi)c_\varphi - G_{nx}(rc_\varphi, b + rs_\varphi)s_\varphi\right] r\mathrm{d}\varphi \tag{51}$$

and

$$\mathcal{Q}(\mathbf{G}_n) = \int\limits_{\pi-\lambda}^{2\pi+\lambda} \left[G_{ny}(c_\varphi, s_\varphi)c_\varphi - G_{nx}(c_\varphi, s_\varphi)s_\varphi\right] \mathrm{d}\varphi\,, \tag{52}$$

where, as before, $c_\varphi \equiv \cos\varphi$ and $s_\varphi \equiv \sin\varphi$ and we used the fact that along the arc of a circle,

$$\mathrm{d}\mathbf{r} = -rs_\varphi\, \mathrm{d}\varphi\, \hat{\mathbf{x}} + rc_\varphi\, \mathrm{d}\varphi\, \hat{\mathbf{y}}\,. \tag{53}$$

In Equations (51) and (52), $\mathcal{P}(\mathbf{G}_n)$ is the line integral along the arc of the occultor and $\mathcal{Q}(\mathbf{G}_n)$ is the line integral along the arc of the occulted body.

As cumbersome as the Green's basis (Equation 30) may appear, the reason we introduced it is that its anti-exterior derivatives are conveniently simple. It can be easily shown that one possible solution to Equation (48) is

$$\mathbf{G}_n = \begin{cases} x^{\frac{\mu+2}{2}} y^{\frac{\nu}{2}}\, \hat{\mathbf{y}} & \nu \text{ even} \\[1em] \dfrac{1-z^3}{3(1-z^2)}(-y\,\hat{\mathbf{x}} + x\,\hat{\mathbf{y}}) & \nu = \mu = 1 \\[1em] x^{l-2} z^3\, \hat{\mathbf{x}} & \nu \text{ odd},\ \mu = 1,\ l \text{ even} \\[1em] x^{l-3} y z^3\, \hat{\mathbf{x}} & \nu \text{ odd},\ \mu = 1,\ l \text{ odd} \\[1em] x^{\frac{\mu-3}{2}} y^{\frac{\nu-1}{2}} z^3\, \hat{\mathbf{y}} & \text{otherwise,} \end{cases} \tag{54}$$

where l and m are given by Equation (15) and μ and ν are given by Equation (25). Solving the occultation problem is therefore a matter of evaluating the primitive integrals of $\mathbf{G}_n$ (Equations 51 and 52). The solutions are in general tedious, but they are all analytic, involving sines, cosines, and complete elliptic integrals. In the Appendix we derive recurrence relations to quickly compute these. We note, in particular, that all solutions involve complete elliptic integrals of the *same* argument, so that the elliptic integrals need only be evaluated once for a map of arbitrary order,

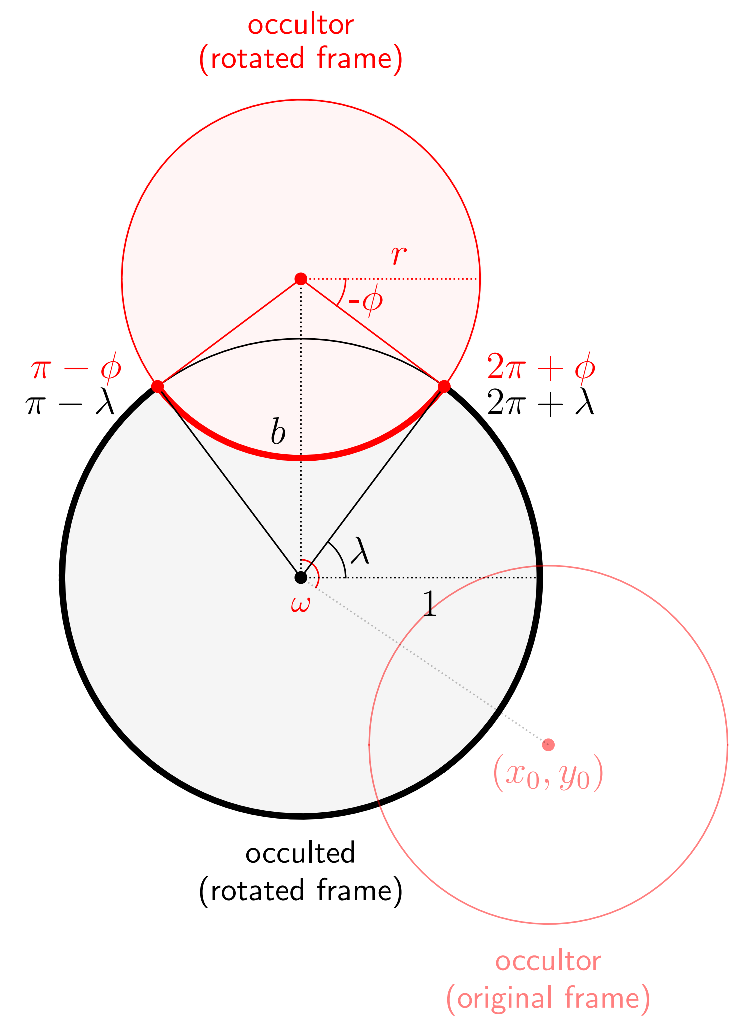

Figure 2. Geometry of the occultation problem. The occulted body is centered at the origin and has unit radius, while the occultor is centered at (x_0, y_0) and has radius r. We first rotate the two bodies about the origin through an angle $\theta = {}^{\pi}/_{2} - \text{arctan2}(y_0, x_0)$ so the problem is symmetric about the y-axis. In this frame, the occultor is located at $(0, b)$, where $b = \sqrt{x_0^2 + y_0^2}$ is the impact parameter. The arc of the occultor that overlaps the occulted body (thick red curve) now extends from $\pi - \phi$ to $2\pi + \phi$, measured from the center of the occultor. The arc of the occulted body that is visible during the occultation (thick black curve) extends from $\pi - \lambda$ to $2\pi + \lambda$, measured from the origin. These are the curves along which the primitive integrals (Equations 51 and 52) are evaluated. The angles ϕ and λ are given by Equations (45) and (46) and extend from $-{}^{\pi}/_{2}$ to ${}^{\pi}/_{2}$. When the occultor is completely within the disk of the occulted body, we define $\phi = \lambda = {}^{\pi}/_{2}$.

greatly improving the evaluation speed and the scalability of the problem to high order.

6.3. *Summary*

Here we briefly summarize how to analytically compute the flux during an occultation of a body whose specific intensity profile is described by a sum of spherical harmonics. Given a body of unit radius with a surface map described by the vector of spherical harmonic coefficients $\mathbf{y}$ (Equation 13), occulted by another body of radius r centered at the point (x_0, y_0), we must:

1. Compute the rotation matrix $\mathbf{R}$ to rotate the map to the correct viewing orientation, which may be specified by the Euler angles α, β, and γ (§4.1) or by an axis $\mathbf{u}$ and an angle θ (§4.2).

2. Compute the rotation matrix $\mathbf{R'}$ to rotate the map by an angle ω about the $+z$-axis (Equation 44) so the center of the occultor is a distance $b = \sqrt{x_0^2 + y_0^2}$ along the $+y$-axis from the center of the occulted body.

3. Compute the change-of-basis matrix $\mathbf{A}$ (§5) to convert our vector of spherical harmonic coefficients to a vector of polynomial coefficients in the Green's basis (Equation 30). Since $\mathbf{A}$ is the same for all occultations, this matrix may be pre-computed to improve computational speed.

4. Compute the solution vector $\mathbf{s}$ (Equation 50), with $\mathcal{P}(\mathbf{G}_n)$ and $\mathcal{Q}(\mathbf{G}_n)$ given by Equations (A10) and (A11). Note that s_2 is special and must be computed separately (Equation A1).

Given these quantities, the total flux during an occultation is then just

$$\boxed{F = \mathbf{s}^\mathsf{T} \mathbf{A} \, \mathbf{R'} \, \mathbf{R} \, \mathbf{y}}. \tag{55}$$

7. THE **STARRY** CODE PACKAGE

The starry code package provides code to analytically compute light curves for celestial bodies using the formalism developed in this paper. starry is coded in C for speed and wrapped in Python for quick and easy light curve calculations. The code may be installed by running the following in a terminal:

```
git clone https://github.com/rodluger/starry.git
cd starry
python setup.py develop
```

To begin using starry, execute the following in a Python environment:

```
from starry import starry
```

7.1. *Creating a map*

A starry map is a vector of spherical harmonic coefficients, indexed by increasing order and degree, as in Equation (13). We can create a map of spherical harmonics up to order $l_{\rm max} = 5$ by typing

```
y = starry(5)
```

The result is an array of spherical harmonics coefficients, set to zero by default. Say our surface map is given by the function

$$I(x, y) = -2Y_{5,-3}(x, y) + 2Y_{5,0}(x, y) + Y_{5,4}(x, y)\,. \tag{56}$$

To instantiate this map, we set the corresponding coefficients in y:

```
y[5, -3] = -2
y[5, 0] = 2
y[5, 4] = 1
```

The map may be visualized by rendering it on a grid:

```
I = y.render(u=None, theta=None)
```

where I is a 2-dimensional array of specific intensity values. Optionally, the user may provide an axis array u and an angle theta to specify the orientation of the map. Plotting this map with successive rotations about $\hat{\mathbf{x}}$ yields

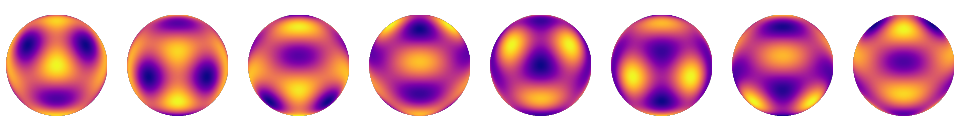

Alternatively, users may provide the path to an image file of the surface map on a rectangular latitude-longitude grid or a ring-ordered Healpix map array:

```
y = starry(10, image=None)
```

starry uses the map2alm() function of the healpy package to find the expansion of the map in terms of spherical harmonics. In Figure 3 we show a simplified two-color map of the cloudless Earth and its corresponding starry instance for $l_{\rm max} = 10$, rotated successively about $\hat{\mathbf{x}}$.

7.2. *Computing phase curves*

Once a map is instantiated, it is easy to compute its phase curve, F:

```
F = y.flux(u=u, theta=theta)
```

where u is the axis of rotation and theta is an array of angles at which to compute the flux. Note that rotations performed by flux() are not cumulative; instead, all angles

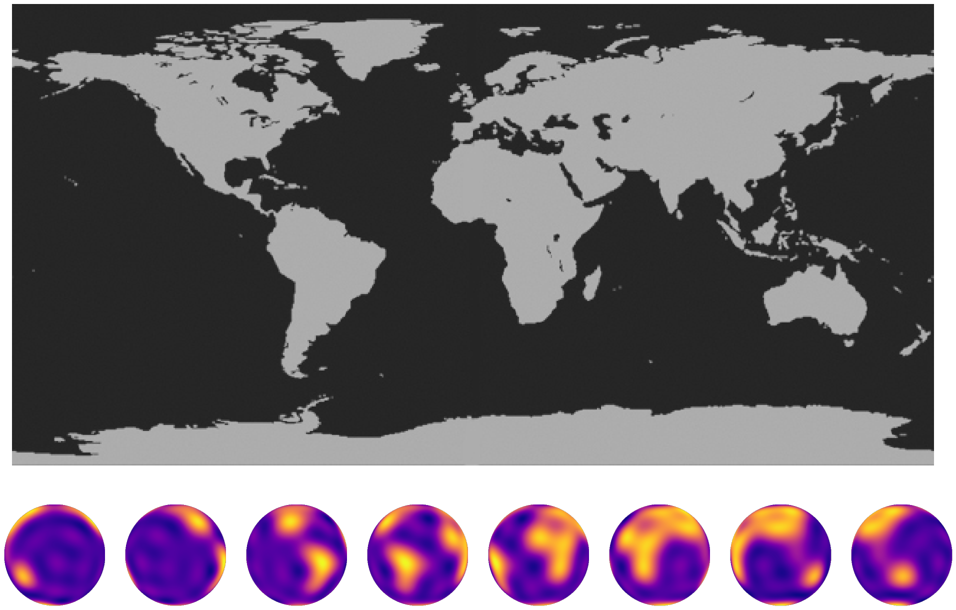

Figure 3. A simplified two-color map of the cloudless Earth (top) and the corresponding tenth-order spherical harmonic expansion, rotated about $\hat{\mathbf{y}}$ (bottom).

should be specified relative to the original, unrotated map frame. In the top panel of Figure 4 we plot phase curves for all spherical harmonics up to $l_{\mathrm{max}} = 6$ for rotation about $\hat{\mathbf{x}}$ (blue) and $\hat{\mathbf{y}}$ (orange). As discussed by Cowan et al. (2013), harmonics with odd $l > 1$ and those with $m < 0$ (not plotted) are in the null space and therefore do not exhibit phase variations.

As a second example, we can compute the phase curve of the simplified Earth model (Figure 3) for rotation about $\hat{\mathbf{y}}$ (its actual spin axis) by executing

```
theta = np.linspace(0, 2 * np.pi, 100)
F = y.flux(u=[0, 1, 0], theta=theta)
```

assuming the numpy package is imported. The variable F is an array of flux values computed from Equation (38); we plot this in Figure 5, alongside the phase curves due to each of the seven individual continents.

7.3. *Computing occultation light curves*

Occultation light curves are similarly easy to compute:

```
F = y.flux(u=u, theta=theta, x0=x0, y0=y0, r=r)
```

where u and theta are the same as above, and x0, y0, and r are the occultor parameters (x position, y position, and radius, all in units of the occulted body's radius), which may be either constants or arrays.

In the bottom panel of Figure 4 we plot occultation light curves for the spherical harmonics with $m \geq 0$ up to $l_{\mathrm{max}} = 6$. The occultor has radius $r = 0.3$ and moves at a constant speed along the x direction at $y_0 = 0.25$ (blue curves) and $y_0 = 0.75$

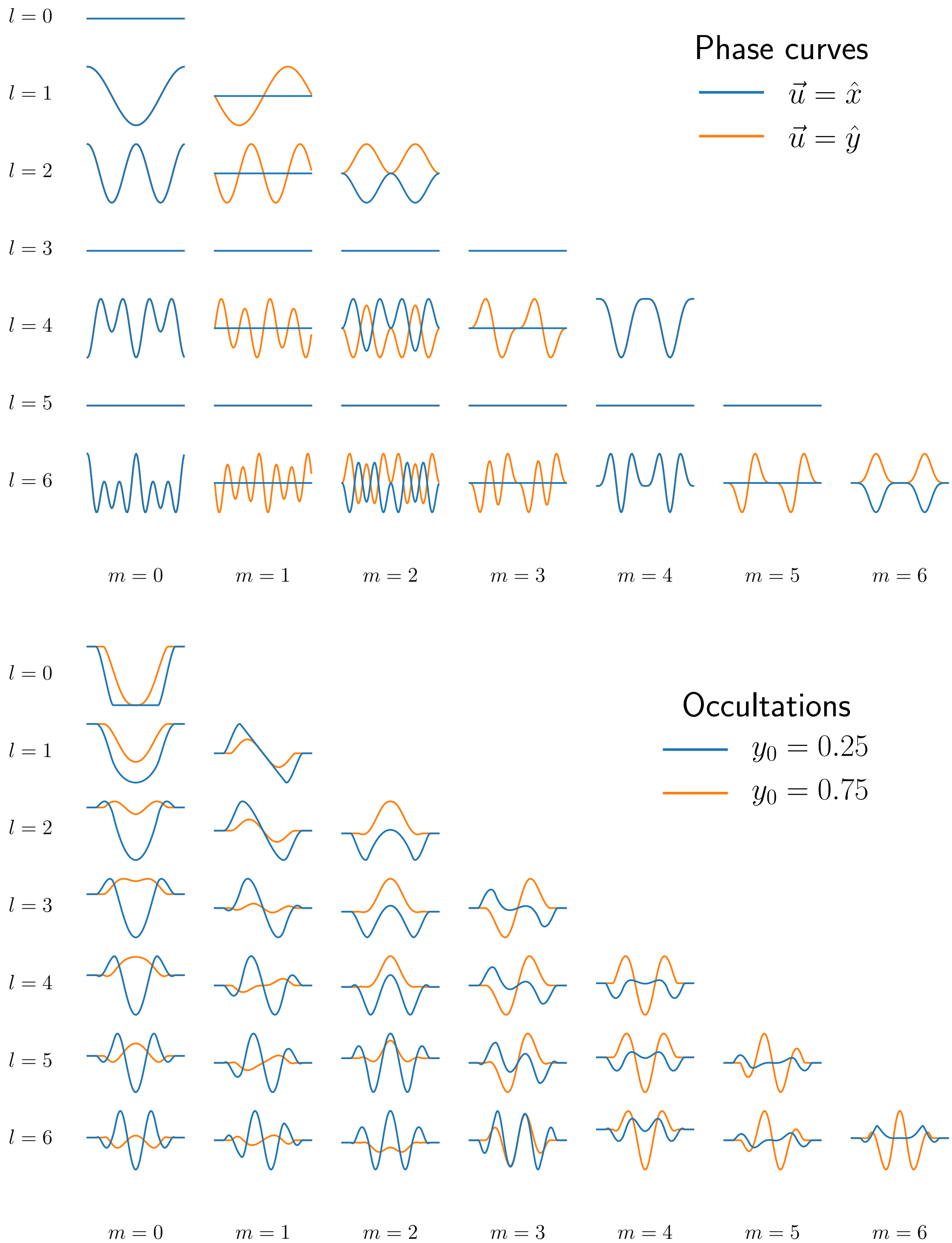

Figure 4. *Top:* Phase curves for the first several spherical harmonics with degree $m \geq 0$ rotated about the x-axis (blue) and about the y-axis (orange). Odd harmonics with $l > 1$ and harmonics with $m < 0$ are in the phase curve null space (Cowan et al. 2013). *Bottom:* Occultation light curves for the same set of spherical harmonics. An occultor of radius $r = 0.3$ transits the body along the $+x$ direction at $y_0 = 0.25$ (blue) and $y_0 = 0.75$ (orange).

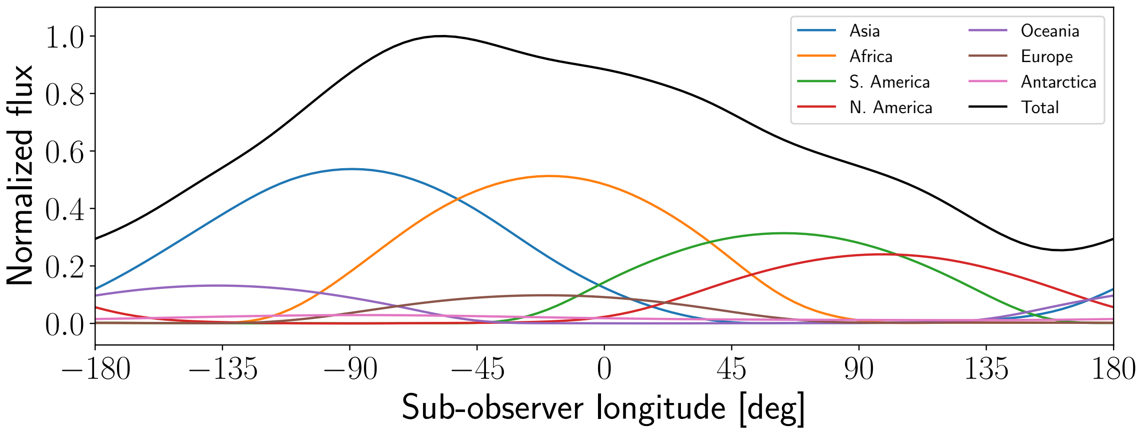

Figure 5. Phase curve for the Earth rotating about its axis, computed from the $l_{\max} = 10$ expansion from Figure 3. The full phase curve is shown in black, and the flux due to each of the seven continents is shown as the colored curves (see legend).

(orange curves). The light curve of any body undergoing such an occultation can be expressed as a weighted sum of these light curves. Note that because the value of individual spherical harmonics can be negative, an increase in the flux is visible at certain points during the occultation; however, this would of course not occur for any physical map constructed from a linear combination of the spherical harmonics. Note also that unlike in the case of phase curves, there is no null space for occultations, as all spherical harmonics (including those with $m < 0$, which are not shown) produce a flux signal during occultation.

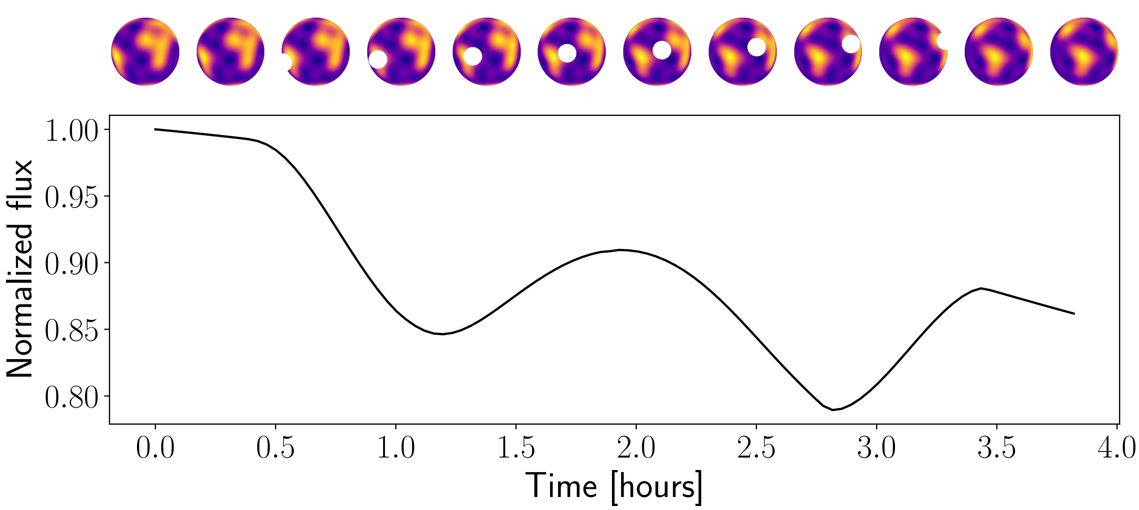

Figure 6. Occultation light curve for the Moon transiting the rotating Earth, computed from the $l_{\max} = 10$ expansion from Figure 3. The two largest dips are due to the occultations of South America (left) and Africa (right).

To further illustrate the code, we return to our spherical harmonic expansion of the Earth. Figure 6 shows an occultation light curve computed for a hypothetical transit of the Earth by the Moon. The occultation lasts about four hours, during which time the sub-observer point rotates from Africa to South America, causing a steady flux decrease as the Pacific Ocean rotates into view. The occultation is double-dipped: one dip due to the occultation of South America, and one dip due to the occultation of Africa.

7.4. *Computing transit light curves*

The formalism developed in this paper can easily be extended to the case of occultations (transits) of limb-darkened stars by noting that any radially symmetric specific intensity profile can be expressed as a sum over the $m = 0$ spherical harmonics (see Figure 1). In particular, the radial intensity profile of a quadratically limb-darkened star,

$$I(\mu) = 1 - u_1(1-\mu) - u_2(1-\mu)^2\,, \tag{57}$$

where $\mu = z = \sqrt{1 - x^2 - y^2}$ and u_1 and u_2 are the limb darkening coefficients, can be written in terms of spherical harmonics by re-writing Equation (57) as

$$I(\mu) = (1 - u_1 - 2u_2) + (u_1 + 2u_2)z + u_2 x^2 + u_2 y^2\,. \tag{58}$$

Inverting Equation (28) to express this polynomial in the basis of spherical harmonics, we have

$$I(x,y) = \frac{2\sqrt{\pi}}{3}(3 - 3u_1 + 4u_2)\,Y_{0,0} + \frac{2\sqrt{\pi}}{\sqrt{3}}(u_1 + 2u_2)\,Y_{1,0} - \frac{4\sqrt{\pi}}{3\sqrt{5}}u_2\,Y_{2,0}\,. \tag{59}$$

Thus, quadratic limb darkening can be expressed exactly as the sum of the first three $m = 0$ spherical harmonics. For convenience, this is implemented in starry:

```
y = starry(2, u1=u1, u2=u2)
```

although users may also specify the coefficients in Equation (59) as in §7.1. Figure 7 shows a transit light curve computed with starry for $u_1 = 0.4, u_2 = 0.26$. The planet/star radius ratio is $r = 0.1$ and the planet transits at impact parameter $b = 0.5$. For comparison, we also compute the flux with batman (Kreidberg 2015) and by a high precision numerical integration of the surface integral of Equation (57). The error on the transit depth for starry flux is less than 10^{-5} parts per million everywhere in the light curve.

7.5. *Photodynamics*

Integrate with planetplanet for easy photodynamics. todo

7.6. *Benchmarks*

Add benchmarks here. Discuss Python tests. todo

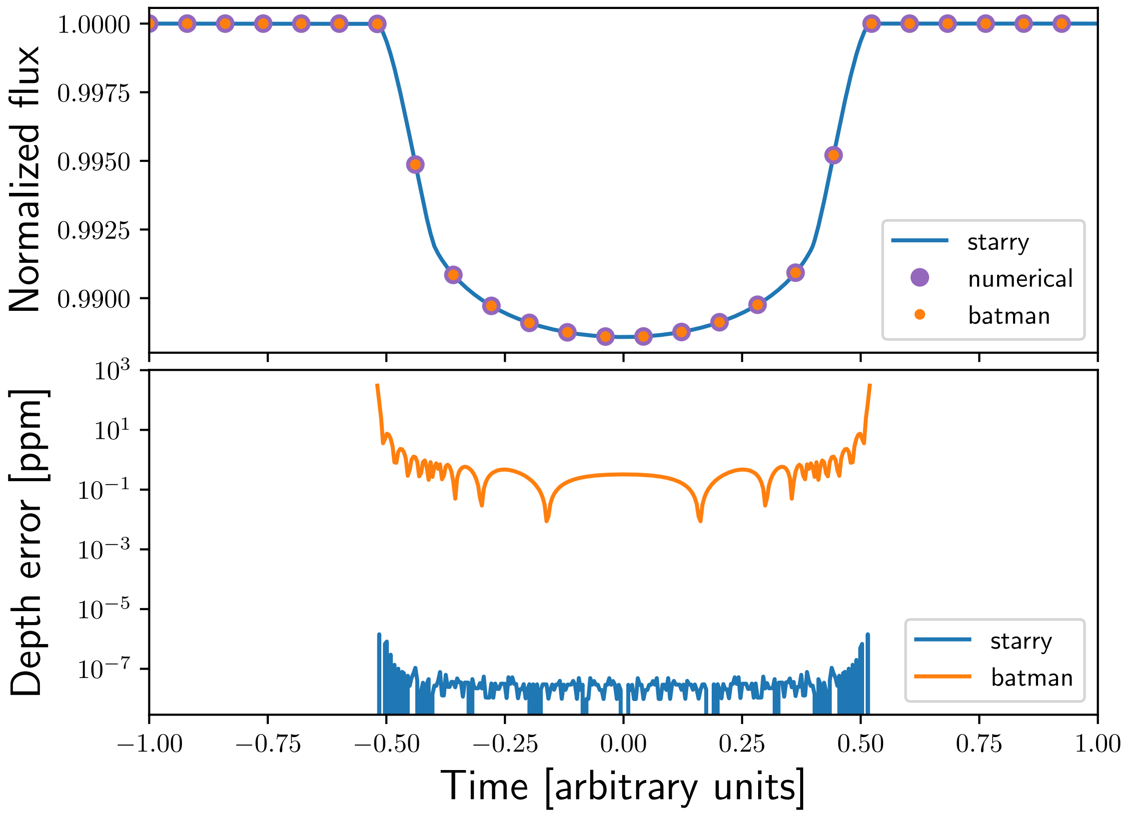

Figure 7. Sample transit light curve for a planet ($r = 0.1$) transiting a quadratically limb-darkened star ($u_1 = 0.4, u_2 = 0.26$). The top panel shows the starry (blue curve) and batman (orange dots) light curves, as well as a light curve generated by a high precision direct numerical integration of the surface integral (purple dots). The bottom panel shows the fractional error on the transit depth in parts per million relative to the numerical solution for starry (blue) and batman (orange).

7.7. *Speed tests*

Discuss speed tests here once I code everything up in C.

todo

8. CONCLUSIONS

Write an awesome conclusions section.

todo

APPENDIX

A. COMPUTING THE SOLUTION VECTOR s_n

Here we seek a solution to Equation (50), which gives the total flux during an occultation of the n^{th} term in the Green's basis (Equation 30). The primitive integrals $\mathcal{P}$ and $\mathcal{G}$ in that equation are given by Equations (51) and (52), with $\mathbf{G}_n$ defined in Equation (54). Note that all of the terms in Equation (54), with the exception of the $\mu = \nu = 1$ case, are simple polynomials in x, y, and z, which facilitates their integration. The $\mu = \nu = 1$ term (corresponding to the $n = 2$ term in the Green's basis) is more difficult to integrate, but an analytic solution exists (Pál 2012). It is, however, more convenient to note that this term corresponds to a surface map given by the polynomial $I(x,y) = \tilde{g}_2(x,y) = \sqrt{1-x^2-y^2}$, which is the same function used to model linear limb darkening in stars (Mandel & Agol 2002). We therefore evaluate this term separately in Appendix A.1 below, followed by the general term in Appendix A.2.

A.1. *Linear limb darkening ($n = 2$)*

From Mandel & Agol (2002), the total flux visible during the occultation of a body whose surface map is given by $I(x,y) = \sqrt{1-x^2-y^2}$ is

$$s_2 = \frac{2}{3\pi}\left(1 - \frac{3\Lambda}{2} - \Theta(r-b)\right) \tag{A1}$$

where $\Theta(\cdot)$ is the Heaviside step function and

$$\Lambda = \begin{cases} -\frac{2}{3}\left(1-r^2\right)^{\frac{3}{2}} & b = 0 \\ \frac{1}{9\pi\sqrt{br}}\Bigg[(-3+12r^2-10b^2r^2-6r^4+\xi)K(k^2) \\ \qquad - 2\xi E(k^2) + 3\left(\frac{b+r}{b-r}\right)\Pi\left(1-\frac{1}{(b-r)^2}, k^2\right)\Bigg] & k^2 < 1 \\ \frac{1}{9\pi\sqrt{(1-b+r)(1+b-r)}}\Bigg[2\left(1-5b^2+r^2+(r^2-b^2)^2\right)K\left(\frac{1}{k^2}\right) \\ \qquad - 2\xi k^2 E\left(\frac{1}{k^2}\right) \\ \qquad + 3\left(\frac{b+r}{b-r}\right)\Pi\left(\frac{1}{k^2-\frac{1}{4br}}, \frac{1}{k^2}\right)\Bigg] & k^2 \geq 1 \end{cases} \tag{A2}$$

with

$$\xi = 2br(4-7r^2-b^2) \tag{A3}$$

and

$$k^2 = \frac{1-r^2-b^2+2br}{4br}\,. \tag{A4}$$

In the expressions above, $K(\cdot)$, $E(\cdot)$, and $\Pi(\cdot)$ are the complete elliptic integrals of the first, second kind, and third kind, respectively, defined as

$$\begin{aligned}
K(k^2) &\equiv \int_0^{\frac{\pi}{2}} \frac{\mathrm{d}\varphi}{\sqrt{1-k^2\sin^2\varphi}} \\
E(k^2) &\equiv \int_0^{\frac{\pi}{2}} \sqrt{1-k^2\sin^2\varphi}\,\mathrm{d}\varphi \\
\Pi(n^2,k^2) &\equiv \int_0^{\frac{\pi}{2}} \frac{\mathrm{d}\varphi}{(1-n^2\sin^2\varphi)\sqrt{1-k^2\sin^2\varphi}}\,.
\end{aligned} \tag{A5}$$

A.2. *All other terms*

We evaluate all other terms in s_n by integrating the primitive integrals of $\mathbf{G}_n$. These are given by

$$\mathcal{P}(\mathbf{G}_n) = \begin{cases}
+\displaystyle\int\limits_{\pi-\phi}^{2\pi+\phi} (rc_\varphi)^{\frac{\mu+2}{2}}(b+rs_\varphi)^{\frac{\nu}{2}} rc_\varphi\,\mathrm{d}\varphi & \nu\ \text{even} \\
-\displaystyle\int\limits_{\pi-\phi}^{2\pi+\phi} (rc_\varphi)^{l-2}(1-r^2-b^2-2brs_\varphi)^{\frac{3}{2}} rs_\varphi\,\mathrm{d}\varphi & \nu\ \text{odd},\ \mu=1,\ l\ \text{even} \\
-\displaystyle\int\limits_{\pi-\phi}^{2\pi+\phi} (rc_\varphi)^{l-3}(b+rs_\varphi)(1-r^2-b^2-2brs_\varphi)^{\frac{3}{2}} rs_\varphi\,\mathrm{d}\varphi & \nu\ \text{odd},\ \mu=1,\ l\ \text{odd} \\
+\displaystyle\int\limits_{\pi-\phi}^{2\pi+\phi} (rc_\varphi)^{\frac{\mu-3}{2}}(b+rs_\varphi)^{\frac{\nu-1}{2}}(1-r^2-b^2-2brs_\varphi)^{\frac{3}{2}} rc_\varphi\,\mathrm{d}\varphi & \text{otherwise}
\end{cases} \tag{A6}$$

and

$$\mathcal{Q}(\mathbf{G}_n) = \begin{cases}
+\displaystyle\int\limits_{\pi-\lambda}^{2\pi+\lambda} c_\varphi^{\frac{\mu+2}{2}} s_\varphi^{\frac{\nu}{2}} c_\varphi\,\mathrm{d}\varphi & \nu\ \text{even} \\
0 & \text{otherwise,}
\end{cases} \tag{A7}$$

where we have used the fact that the line integral of any function proportional to z taken along the limb of the occulted planet (where $z = \sqrt{1 - x^2 - y^2} = 0$) is zero. For convenience, let us introduce the expressions

$$\mathcal{H}^{\nu}_{u,n}(\xi, \beta, \rho) = \begin{cases} \displaystyle\int\limits_{\pi-\xi}^{2\pi+\xi} c_\varphi^u s_\varphi^n \, \mathrm{d}\varphi & \nu \text{ even} \\ \\ \displaystyle\int\limits_{\pi-\xi}^{2\pi+\xi} c_\varphi^u s_\varphi^n (1 - \rho^2 - \beta^2 - 2\beta\rho s_\varphi)^{\frac{3}{2}} \, \mathrm{d}\varphi & \nu \text{ odd} \end{cases} \tag{A8}$$

and

$$\mathcal{I}^{\nu}_{u,v}(\xi, \beta, \rho) = \sum_{n=0}^{v} \binom{v}{n} \left(\frac{\beta}{\rho}\right)^{v-n} \mathcal{H}^{\nu}_{u,n}(\xi, \beta, \rho)\,. \tag{A9}$$

With some algebra, we may therefore write

$$\mathcal{P}(\mathbf{G}_n) = \begin{cases} r^{l+2} \mathcal{I}^{\nu}_{\frac{\mu+4}{2}, \frac{\nu}{2}}(\phi, b, r) & \nu \text{ even} \\ \\ b r^{l-2} \mathcal{I}^{\nu}_{l-2,0}(\phi, b, r) - r^{l-1} \mathcal{I}^{\nu}_{l-2,1}(\phi, b, r) & \nu \text{ odd}, \ \mu = 1, \ l \text{ even} \\ \\ b r^{l-2} \mathcal{I}^{\nu}_{l-3,1}(\phi, b, r) - r^{l-1} \mathcal{I}^{\nu}_{l-3,2}(\phi, b, r) & \nu \text{ odd}, \ \mu = 1, \ l \text{ odd} \\ \\ r^{l-1} \mathcal{I}^{\nu}_{\frac{\mu-1}{2}, \frac{\nu-1}{2}}(\phi, b, r) & \text{otherwise} \end{cases} \tag{A10}$$

proof

and

$$\mathcal{Q}(\mathbf{G}_n) = \begin{cases} \mathcal{I}^{\nu}_{\frac{\mu+4}{2}, \frac{\nu}{2}}(\lambda, 0, 1) & \nu \text{ even} \\ \\ 0 & \text{otherwise.} \end{cases} \tag{A11}$$

proof

The solution to the occultation problem is therefore a matter of finding expressions for $\mathcal{H}^{\nu}_{u,n}$ (Equation A8):

Case 1: ν even

For even ν, $\mathcal{H}^{\nu}_{u,n}$ evaluates to terms containing only sines and cosines of ξ. Pál (2012) derived simple recurrence relations for these terms:

$$\mathcal{H}^{\nu}_{u,n}(\xi,\beta,\rho) = \begin{cases} 0 & u \text{ odd} \\ 2\xi + \pi & u = n = 0 \\ -2\cos\xi & u = 0, n = 1 \\ \dfrac{2}{u+n}(\cos\xi)^{u-1}(\sin\xi)^{n+1} + \dfrac{u-1}{u+n}\mathcal{H}^{\nu}_{u-2,n}(\xi,\beta,\rho) & u \geq 2 \\ -\dfrac{2}{u+n}(\cos\xi)^{u+1}(\sin\xi)^{n-1} + \dfrac{n-1}{u+n}\mathcal{H}^{\nu}_{u,n-2}(\xi,\beta,\rho) & n \geq 2\,. \end{cases} \tag{A12}$$

proof

Case 2: ν odd

When ν is odd, $\mathcal{Q}(\mathbf{G}_n) = 0$ and we need only compute $\mathcal{P}(\mathbf{G}_n)$, for which $\xi = \phi$, $\beta = b$, and $\rho = r$. However, because of the term raised to the $3/2$ power in Equation (A8) for odd ν, the integral becomes significantly more difficult to compute. With some tedious algebraic manipulation, and using recurrence relations for expressions with integrands of the form $\cos^p\varphi\sin^q\varphi(1-\chi^2\sin^2\varphi)^{\frac{3}{2}}$ (Gradshtein & Ryzhik 1994), we may write

$$\mathcal{H}^{\nu}_{u,n}(\phi,b,r) = 2^{u+3}(br)^{\frac{3}{2}}\sum_{i=0}^{n}\binom{n}{i}(-1)^{i-n-u}\,\mathcal{J}_{u+2i,u+2n-2i}(k^2) \tag{A13}$$

where

$$\mathcal{J}_{p,q}(k^2) = \begin{cases} 0 & p \text{ odd or } q \text{ odd} \\ \dfrac{d_1\mathcal{J}_{p,q-2}(k^2) + d_2\mathcal{J}_{p,q-4}(k^2)}{p+q+3} & q \geq 4 \\ \dfrac{d_3\mathcal{J}_{p-2,q}(k^2) + d_4\mathcal{J}_{p-4,q}(k^2)}{p+q+3} & p \geq 4 \end{cases} \tag{A14}$$

with

$$
\begin{aligned}
d_1 &= q + 2 + (p + q - 2)(1 - k^2) \\
d_2 &= (3 - q)(1 - k^2) \\
d_3 &= 2p + q - (p + q - 2)(1 - k^2) \\
d_4 &= (3 - p) + (p - 3)(1 - k^2)
\end{aligned} \tag{A15}
$$

and k^2 defined as in Equation (A4). These recurrence relations require four initial conditions:

$$
\begin{aligned}
\mathcal{J}_{0,0}(k^2) &= \frac{8 - 12k^2}{3}\mathcal{E}_1(k^2) + \frac{-8 + 16k^2}{3}\mathcal{E}_2(k^2) \\
\mathcal{J}_{0,2}(k^2) &= \frac{8 - 24k^2}{15}\mathcal{E}_1(k^2) + \frac{-8 + 28k^2 + 12k^4}{15}\mathcal{E}_2(k^2) \\
\mathcal{J}_{2,0}(k^2) &= \frac{32 - 36k^2}{15}\mathcal{E}_1(k^2) + \frac{-32 + 52k^2 - 12k^4}{15}\mathcal{E}_2(k^2) \\
\mathcal{J}_{2,2}(k^2) &= \frac{32 - 60k^2 + 12k^4}{105}\mathcal{E}_1(k^2) + \frac{-32 + 76k^2 - 36k^4 + 24k^6}{105}\mathcal{E}_2(k^2)\,,
\end{aligned} \tag{A16}
$$

where

$$
\mathcal{E}_1(k^2) = \begin{cases} (1 - k^2)K\left(k^2\right) & k^2 < 1 \\ \dfrac{1 - k^2}{\sqrt{k^2}}K\left(\dfrac{1}{k^2}\right) & k^2 \geq 1 \end{cases} \tag{A17}
$$

and

$$
\mathcal{E}_2(k^2) = \begin{cases} E\left(k^2\right) & k^2 < 1 \\ \sqrt{k^2}E\left(\dfrac{1}{k^2}\right) + \dfrac{1 - k^2}{\sqrt{k^2}}K\left(\dfrac{1}{k^2}\right) & k^2 \geq 1\,. \end{cases} \tag{A18}
$$

Interestingly, the elliptic integrals in the expressions above are exactly the same as the ones used to evaluate the s_2 term (Equation A2), so these need only be evaluated *once* when computing the occultation flux of a map of arbitrary order. Thanks to the recurrence relations, all other operations required to evaluate the integrals for odd μ are elementary, making the computation of s_n fast.

Note, finally, that the expressions above diverge when $b = 0$, since $k^2 \to \infty$. In this case, the integral in Equation (A8) simplifies:

$$\mathcal{H}_{u,n}^{\nu}(\phi, 0, r) = (1 - r^2)^{\frac{3}{2}} \mathcal{H}_{u,n}^{\nu+1}(\phi, 0, r) \tag{A19}$$

with $\mathcal{H}_{u,n}^{\nu+1}$ given by Equation (A12).

REFERENCES

Collado, J. R. A., et al. 1989, Computer Physics Communications, 52, 323

Cowan, N. B., et al. 2013, MNRAS, 434, 2465

Gradshtein, I., & Ryzhik, I. 1994, Table of Integrals, Series, and Products, 5th edn., ed. A. Jeffrey (Academic Press)

Kreidberg, L. 2015, PASP, 127, 1161

Mandel, K., & Agol, E. 2002, ApJL, 580, L171

Pál, A. 2012, MNRAS, 420, 1630

Steinborn, E., & Ruedenberg, K. 1973, 7, 1

Table 1. Symbols used in this paper

Symbol	Definition	Reference
A_{lm}	Legendre function normalization	Equation (5)
$\mathbf{A}$	Change of basis matrix: Y_{lm}s to Green's polynomials	Equation (34)
$\mathbf{A_1}$	Change of basis matrix: Y_{lm}s to polynomials	§5.1
$\mathbf{A_2}$	Change of basis matrix: polynomials to Green's polynomials	§5.2
b	Impact parameter in units of occulted body's radius	§6
B^{jk}_{lm}	Spherical harmonic normalization	Equation (8)
$c.$	$\cos(\cdot)$	
C^k_{pq}	Expansion coefficient for $z(x,y)$	Equation (10)
$\mathbf{D}^l$	Rotation matrix for the complex spherical harmonics of order l	Equation (18)
$\mathbf{D}\wedge$	Exterior derivative	Equation (49)
$E(\cdot)$	Complete elliptic integral of the second kind	Equation (A5)
$\mathcal{E}_1$	First elliptic function	Equation (A17)
$\mathcal{E}_2$	Second elliptic function	Equation (A18)
F	Total flux seen by observer	Equation (55)
$\tilde{\mathbf{g}}$	Green's basis	Equation (30)
$\mathbf{g}$	Vector in the basis $\tilde{\mathbf{g}}$	
$\mathbf{G}_n$	Anti-exterior derivative of the n^{th} term in the Green's basis	Equation (54)
$\mathcal{H}^{\nu}_{u,n}$	Occultation integral	Equation (A8)
I	Specific intensity, $I(x,y)$	Equation (12)
$\mathcal{I}^{\nu}_{u,v}$	Occultation integral	Equation (A9)
j	Dummy index	
$\mathcal{J}_{p,q}$	Occultation integral	Equation (A14)
k	Dummy index	
k^2	Elliptic parameter	Equation (A4)
$K(\cdot)$	Complete Elliptic integral of the first kind	Equation (A5)
l	Spherical harmonic order	Equation (15)
m	Spherical harmonic degree	Equation (15)
n	Surface map vector index, $n = l^2 + l + m$	Equation (14)
p	Dummy index	
$\bar{P}$	Normalized associated Legendre function	Equation (4)
$\tilde{\mathbf{p}}$	Polynomial basis	Equation (24)
$\mathbf{p}$	Vector in the basis $\tilde{\mathbf{p}}$	
$\mathbf{P}$	Cartesian axis-angle rotation matrix	Equation (21)
$\mathcal{P}$	Primitive integral along perimiter of occultor	Equation (51)
q	Dummy index	
$\mathbf{Q}$	Cartesian Euler angle rotation matrix	Equation (22)

Table 1 – continued from previous page

Symbol	Definition	Reference
$\mathcal{Q}$	Primitive integral along perimiter of occulted body	Equation (52)
r	Occultor radius in units of occulted body's radius	§6
$\mathbf{r}$	Phase curve solution vector	Equation (39)
$\mathbf{R}$	Rotation matrix for the real spherical harmonics	Equation (20)
$\mathbf{R}^l$	Rotation matrix for the real spherical harmonics of order l	Equation (17)
$s_\cdot$	$\sin(\cdot)$	
$\mathbf{s}$	Occultation light curve solution vector	Equation (39)
u_1, u_2	Quadratic limb darkening coefficients	Equation (57)
$\mathbf{u}$	Unit vector corresponding to the axis of rotation	§4.2
$\mathbf{U}$	Complex to real spherical harmonics transform matrix	Equation (19)
x	Cartesian coordinate	Equation (2)
y	Cartesian coordinate	Equation (2)
$Y_{l,m}$	Spherical harmonic of order l and degree m	Equation (3)
$\tilde{\mathbf{y}}$	Spherical harmonic basis	Equation (13)
$\mathbf{y}$	Vector in the basis $\tilde{\mathbf{y}}$	
z	Cartesian coordinate, $z = \sqrt{1 - x^2 - y^2}$	Equation (2)
α	Euler angle ($\hat{\mathbf{z}}$ rotation)	§4.1
β	Euler angle ($\hat{\mathbf{y}}$ rotation)	§4.1
γ	Euler angle ($\hat{\mathbf{z}}$ rotation)	§4.1
Γ	Gamma function	
θ	Polar angle	Equation (1)
	Spherical harmonic rotation angle	§4.2
Θ	Heaviside step function	Equation (A2)
λ	Angular position of occultor/occulted intersection point	Equation (46)
Λ	Mandel & Agol (2002) function	Equation (A2)
μ	$l - m$	Equation (25)
ν	$l + m$	Equation (25)
ξ	Function of b and r	A4
$\Pi(\cdot, \cdot)$	Complete elliptic integral of the third kind	Equation (A5)
ϕ	Spherical harmonic azimuthal angle	Equation (1)
	Angular position of occultor/occulted intersection point	Equation (45)
φ	Dummy integration variable	
ω	Angular position of occultor	Equation (44)